SUMMARY OF ALTITUDE PULSE TESTING OF A 100-LB_F LO_2/LCH_4 REACTION CONTROL ENGINE

William M. Marshall and Julie E. Kleinhenz
National Aeronautics and Space Administration
Glenn Research Center
Cleveland, Ohio 44135

ABSTRACT

Recently, liquid oxygen-liquid methane (LO_2/LCH_4) has been considered as a potential "green" propellant alternative for future exploration missions. The Propulsion and Cryogenic Advanced Development (PCAD) project has been tasked by NASA to develop this propulsion combination to enable safe and cost effective exploration missions. To date, limited experience with such combinations exist, and as a result a comprehensive test program is critical to demonstrating the viability of implementing such a system. The NASA Glenn Research Center has conducted a test program of a 100-lb_f (445-N) reaction control engine (RCE) at the center's Altitude Combustion Stand (ACS), focusing on altitude testing over a wide variety of operational conditions. The ACS facility includes a unique propellant conditioning feed system (PCFS) which allows precise control of propellant inlet conditions to the engine. Engine performance as a result of these inlet conditions was examined extensively during the test program. This paper is a companion to the previous specific impulse testing paper, and discusses the pulsed mode operation portion of testing, with a focus on minimum impulse bit (I-bit) and repeatable pulse performance. The engine successfully demonstrated target minimum impulse bit performance at all conditions, as well as successful demonstration of repeatable pulse widths. Some anomalous conditions experienced during testing are also discussed, including a double pulse phenomenon which was not noted in previous test programs for this engine.

INTRODUCTION

To enable future exploration of the moon, Mars, and beyond, next generation propellant systems are being developed. With an emphasis on non-toxic, "green" propellants, LO_2/LCH_4 has risen to the forefront. Liquid methane (LCH_4) is an attractive propellant because it does not require the strict thermal storage requirements of hydrogen (due to its larger density and higher boiling point), nor does it require the rigorous handling protocols of toxic hypergolic propellants. It also has the potential, when paired with liquid oxygen (LO_2), to produce higher specific impulse than either the existing hypergolic or liquid oxygen-kerosene systems. This higher specific impulse and improved storage capability could reduce vehicle mass, since smaller propellant storage and management would be required. Not only is there a potential for decreased vehicle mass, these propellants can also be produced on Mars using local resources. Prior work with this propellant combination is limited, so a goal of the NASA Propulsion and Cryogenic Advanced Development (PCAD) project was to examine the feasibility and performance characteristics of these systems (Refs. 1-3). In particular, there is interest in demonstrating repeatable and reliable ignition of an engine over a wide range of valve inlet temperatures (from liquid-liquid operation to gas-gas operation), especially at vacuum conditions (Refs. 3,4).

To facilitate this, a 100-lb_f (445-N) LO_2/LCH_4 Reaction Control Engine (RCE) was developed by Aerojet Corporation (Ref. 5). In late 2009 and 2010, this engine underwent a series of tests in the Altitude Combustion Stand (ACS) at the NASA Glenn Research Center (Refs. 6,7). A specially designed Propellant Conditioning Feed System (PCFS) was developed to enable precise propellant temperature control. The first test series (Refs. 6,7) at ACS examined specific impulse performance with burn durations up to 7 s. The engine met the $I_{sp,vac}$ goal, achieving an overall average $I_{sp,vac}$ of 305 seconds ±4 percent. Performance improved as propellant temperature increased or mixture ratio decreased, which is believed to be a result of injection and mixing effects (Ref. 7).

Since this type of engine is more likely to operate in a pulsed operation, the next test series focused on impulse bit (I-bit) performance. Propellant inlet temperatures were again varied to the same three target conditions used in the specific impulse tests: Cold (170 °R (94.4 K) LCH_4, 163 °R (90.5 K)

LO_2); Nominal (204 °R (113 K)); Warm (224 °R (124 K)). Mixture ratio, *MR*, (mass flow oxidizer to mass flow fuel) was targeted for 2.5, which is the nominal operating condition. The goals were to prove repeatable ignition and performance, with a target I-bit of 4 lb_f-s, a minimum pulse duration of 80 ms, and operation at a variety of duty cycle conditions. The results of these tests will be discussed here.

FACILITY AND HARDWARE

Before discussing the results of the testing, it is useful to briefly describe the experimental set-up and conditions planned for the test series.

NASA GLENN ACS FACILITY

Altitude testing of the RCE was conducted in the NASA Glenn Altitude Combustion Stand (ACS) facility. This facility was originally part of the NASA Glenn (then NASA Lewis) RETF (B-Stand) facility (Refs. 8-10). The current capabilities of this facility are described in Reference 7. A photograph of the spray cart and test capsule of the ACS facility is shown in Figure 1.

Figure 1.— Photograph of Spray Cart and Test Capsule of ACS Facility

For the current investigation, performance and characterization of the RCE under pulsed mode operation at various propellant inlet temperatures was the primary interest. To accomplish this, propellant conditioning feed systems (PCFS) were incorporated into the facility for control of propellant conditions. One system was dedicated to methane conditioning, while the other was dedicated to oxygen conditioning. Both have been described in detail previously (Refs. 6,7,11,12). The systems were designed to condition each of the propellants to ±5 °R (±2.8 K) of the target condition.

Data acquisition is achieved through a National Instruments™ module (Ref. 13) and timing is controlled by a programmable logic controller (PLC). The module allows for real-time, streaming views of data at nominal sample rates of up to 1000 Hz and multiple computers in the control room allow for quick-view (post-test) processing, providing researchers vital information to rapidly adjust test conditions and prepare for the next test.

Figure 2 shows a schematic of the propellant feed system for the RCE engine, with associated sensor locations. Pressure transducers were diaphragm type transducers with a range of 0 to 500 psi (0 to 3.44 MPa). Critical temperature measurements were made by Class-A resistance temperature detectors (RTD's), to improve precision, and all other temperature measurements were made by either K-type or T-type thermocouples. All instrumentation was sampled at 1000 Hz.

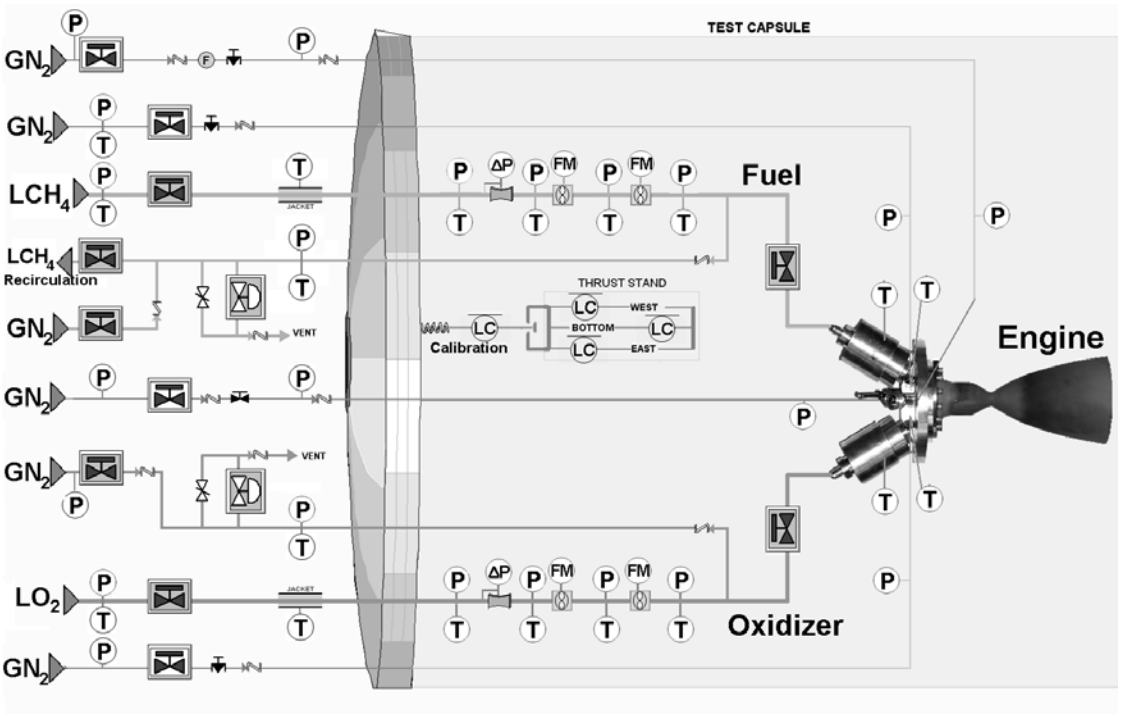

Figure 2.—Feed system schematic for RCE tests in NASA Glenn ACS facility.

Flow rate measurements were calculated using sub-sonic venturi, with pressure and temperature instruments immediately upstream of the venturi for fluid properties (e.g. density) determination. Fluid densities were calculated using the NIST REFPROP program (Ref. 14) A stainless steel-0.100 in. (2.54-mm) throat diameter venturi was used for the liquid oxygen leg, and a 0.080-in. (2.03-mm) throat diameter venturi was used for the liquid methane leg. A 0- to 100-psi (0- to 0.68-MPa) differential pressure transducer was used to measure the differential pressures generated across the venturi. The venturi discharge coefficients (C_d) were measured prior to testing using nitrogen gas for the 0.100-in. (2.54-mm) venturi and liquid water for the 0.080-in. (2.03-mm) venturi. Pairs of dual-rotor turbine flow meters were also installed in series downstream of each venturi (as shown in Figure 2). However, these units did not have a valid calibration at cryogenic conditions, so only the venturi results were used in the data analysis.

The, transient response during the short pulse widths made it difficult to accurately determine or adjust mass flowrates. Therefore, test conditions were based upon steady state set points, and the flowrates and mixture ratios were permitted to vary based upon the transient behavior of the engine feed system. The reported flow rates are time average values over the pulse duration based upon the venturi flow meter measurements

The thrust stand utilized a tri-load cell configuration. The total thrust was the summation of these three load cell measurements, after appropriate zero offsets were applied. Each load cell was a dual bridge design, with a 0- to 100-lb_f (0- to 445-N) range (for a total thrust range of 0- to 300-lb_f (0- to 1334-N)). Calibration of the load cells was accomplished by performing a test pull on the live bed prior to testing, but after the propellant lines and associated hardware had been chilled down in the vacuum chamber (by introducing cryogenics up to the thruster valves). This minimized thrust errors due to thermal flexure of the thrust stand. The resulting calibration factor (K-factor) was applied to the summed load. A final test pull at the end of the day verified the thrust stand calibration did not significantly drift throughout the test day.

RCE HARDWARE DESCRIPTION

The test article for this test series was the Aerojet designed 100-lb_f (445-N) RCE thruster (Refs.5-7,15). This engine is designed to operate at a steady-state mean chamber pressure of 175 psia

(1.2 MPa) and a nominal mixture ratio (*MR*) of 2.5. Details of the engine have been described previously (Refs. 6,7). Only the exciter source and the operating procedures were changed for these pulse tests. A photograph of the engine operating in the ACS facility is shown in Figure 3.

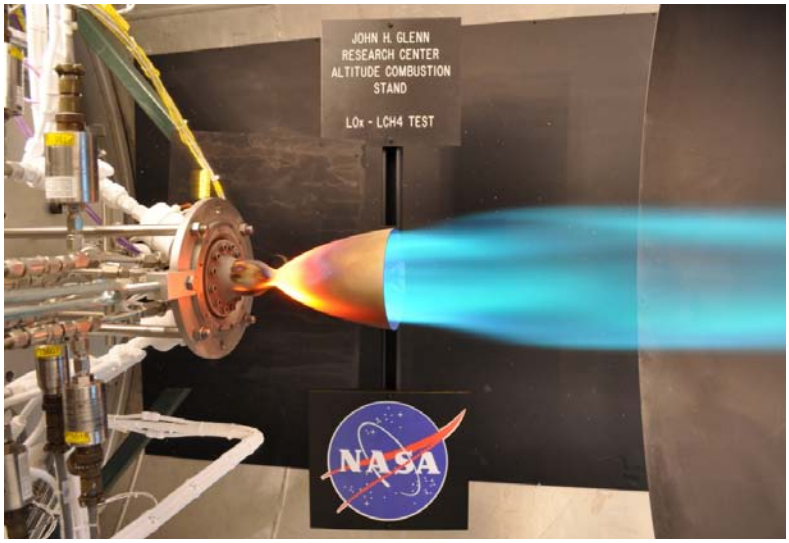

Figure 3.—100-lb_f (445-N) LO_2/LCH_4 RCE operating in NASA Glenn ACS test capsule

The ignition source for the RCE was a spark torch igniter. For initial pulse testing, a Champion (Champion Aerospace, LLC) exciter was used with a spark plug igniter system. This exciter was used in the previous $I_{sp,vac}$ test program. Part way through the test program, however, this exciter was replaced with a similar spark exciter developed by Unison (Unison, LLC) which provided a greater spark rate. At the end of the test series, a compact exciter designed by Unison was also briefly tested. The compact exciter was similar electrically to the Unison exciter, but eliminated the need of an electrical lead between the exciter unit and the spark plug. It performed reliably with no missed ignitions. A photograph of the engine operating with the compact exciter is shown in Figure 4.

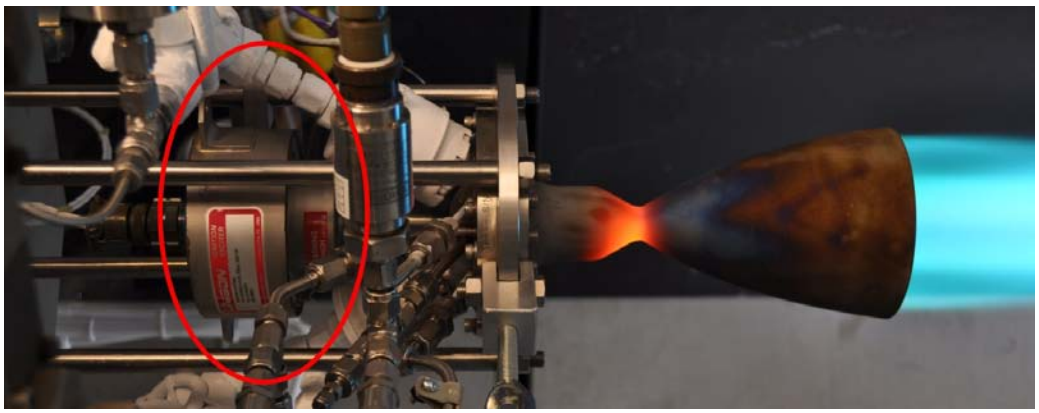

Figure 4.—100-lb_f (445-N) RCE operating with Unison compact exciter (circled)

The injector of the RCE engine was an impinging style design, with fuel film cooling (FFC) and an integrated igniter. Approximately 15 percent of the fuel flow is used for the FFC. The injector was designed to operate at an overall *MR* of 2.48. Surrounding the injector is a series of acoustical cavities. Chamber pressure is measured within one of these cavities.

The combustion chamber and nozzle used for altitude testing was a single piece, radiatively cooled design, made from columbium (niobium) material and coated with an oxidation resistant coating. For all tests described here, the nozzle throat was 0.615-in. (15.6-mm) diameter, with a 6:1 contraction

ratio, 45:1 exit ratio (80 percent bell) and 2.50-in. (63.5-mm) *L'*. The chamber (nozzle) was designed to be bolted to the injector assembly. Since the chamber and nozzles are a single piece, the terms nozzle and chamber are used interchangeably throughout this paper.

TIMING AND PERMISSIVES

Timing for a test at ACS is handled in four zones, which are described in Reference 7. Unless otherwise noted, only Zone 2, the hot fire portion, is discussed in this document. The command timing of Zone 2 encompassed a single pulse, and was then repeated to achieve the desired number of consecutive pulses. The timing of a pulse included a 10-ms LO_2 lead on startup, which was intended to bring both manifolds up to pressure at the same time based on cold propellant flow tests. A 5-psia (0.03-MPa) nitrogen gas purge was introduced through the igniter cavity pressure port and manifold pressure ports between pulses using a check valve. This purge ensured that no combustible gas was trapped in the manifolds between pulses, minimizing the chances for a hard start. The igniter sparks were initiated 20 ms before the LCH_4 flow. Table I lists the command timing with respect to the zone start, and the duration that the valve remains in that commanded state. Thus, a valve (or abort window) that opens at 30 ms, with duration of 50 ms would mean the valve opened at 30 ms into zone 2, and closed at 80 ms into zone 2. The minimum timing resolution of the PLC was 10 ms. At the end of the pulse, the LO_2 valve was closed with the LCH_4 following 40 ms later. This fuel rich shutdown was intended to prevent oxidation on the hot chamber walls.

Table I.—Timing for various pulse widths (EPW's) used in pulse testing

EPW (ms)	Zone 2[a] (ms) [% Duty Cycle]	Spark On/Duration (ms)	Oxygen On/Duration (ms)	Fuel On/Duration (ms)	PCAV Abort Window Start/Duration (ms)
500	980 [50]	230 / 100	240 / 500	250 / 510	350 / 300
100	380 [25]	30 / 100	40 / 110	50 / 140	120 / 20
80	1580 [5]	30 / 90	40 / 90	50 / 120	120 / 10
40	780 [5]	30 / 60	40 / 50	50 / 80	OFF

[a]Zone 2 is repeated for desired number of pulses. Zone 2 is left 20 ms short to account for the PLC delay in repeating the zone.

No attempt was made for a "pre-chill" (pre-flow of liquid oxygen to lower the injector hardware temperature) of the engine prior to start of test. However, the propellant lines were maintained at chilled conditions up to the thruster valves during and between runs by means of trace cooling around the propellant lines. Since no pre-chill was conducted, the injector often started at near ambient temperature (≈500 °R (278 K)). Therefore, there was a considerable transient on startup as the liquid propellant phase changes to gas phase in the manifolds and the manifolds subsequently chill-in.

The electric pulse width (EPW) is the time when both thruster valves are commanded open. In the current study, this is between the opening of the methane valve and when the oxygen valve closes. The duty cycle is the EPW divided by the total run time for a single pulse. Thus, for 80-ms EPW with 5 percent duty cycle, the dwell time between pulses would be 1600 ms (1.6 s). Figure 5 shows a basic timing sequence used for these series of tests. Unless otherwise noted, this timing was maintained for all tests described here.

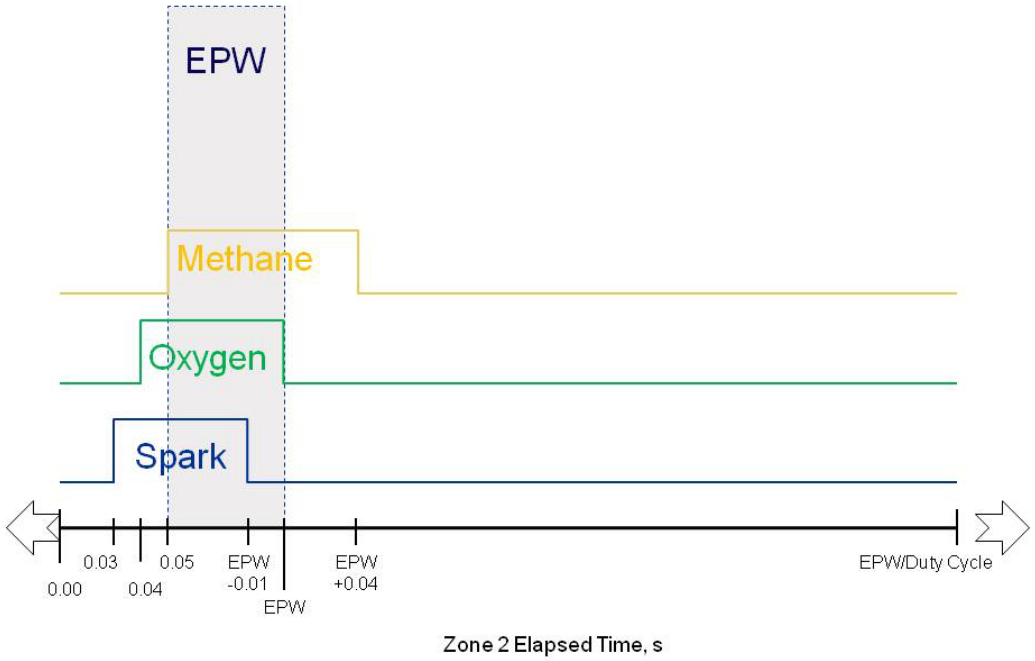

Figure 5.—Basic timing sequence for individual pulses for pulse tests. "EPW" refers to pulse width. A pulse train is accomplished by repeating the above sequence for the given number of pulses.

METHODOLOGY

The test series objectives, the test matrix, and methodology for calculating impulse bit, the primary performance parameter of interest, are described here.

OBJECTIVES OF PULSE TESTING

The objective of pulse testing at NASA GRC was to verify the operation of the engine under pulsed mode operation and to quantify the impulse bit performance at altitude conditions for varying input propellant temperatures. The following technical challenges had to be addressed by the delivered engine (Ref. 5).

(1.) Achieve a minimum impulse bit (MIB) of 4 lb_f-s (17.8 N-s)
(2.) Achieve a minimum EPW of 80 ms or less.
(3.) Achieve a MIB repeatability of ±5 percent after achieving stable temperature
(4.) Operate over 0 to 100 percent duty cycle

Additionally, the performance was characterized over the same matrix of temperature conditions explored in the prior duration testing (Ref. 7). Propellant inlet temperatures were again varied to the same three target conditions used in the specific impulse tests: (1) Cold (170 °R (94.4 K) LCH_4, 163 °R (90.5 K) LO_2), (2) Nominal (204 °R (113 K)) and (3) Warm (224 °R (124 K)).

CALCULATION OF IMPULSE BIT (I-BIT)

Impulse bit, I-bit, is defined as the area under the vacuum thrust curve from the time both propellant valves open until the chamber pressure decays to 10 percent of the rated nominal chamber pressure (17.5 psia (0.12 MPa) for the RCE, which has a 175-psia (1.2-MPa) nominal chamber pressure). This definition is consistent with Aerojet's calculations from previous testing (Ref. 5).

The I-bit integration time was determined by examining the methane manifold pressure and the chamber pressure data sets. A pressure rise in the methane manifold indicated that both valves were open and propellants were actively flowing. Since the end of the integration occurred during the chamber

pressure decay, the peak chamber pressure was first identified. When the pressure reached 17.5 psia (0.12 MPa) (10 percent of the nominal rated value) after this peak, the integration ended. The vacuum thrust was therefore integrated over this period. The result is the impulse bit, in the units of lb_f-s (N-s).

RESULTS AND DISCUSSION

A total of 81 tests were conducted during the pulse test series. Of those 81 tests (which involved 760 ignition events), only four resulted in a non-ignition event, as confirmed by a lack of temperature rise observed in igniter cavity. No conclusive reason for the non-ignitions was evident from the flow conditions or data, as individual spark data (discharge voltage or current, spark pulses, etc.) was not available during this test series. As a result, it was not possible to definitively diagnose the condition of spark energy being delivered to the flow. Further investigation of ignition and spark behavior is planned in a future test series. Figure 6 shows the plot of valve temperatures for the pulse testing program. Note that due to loss of the methane re-circulation pump, methane temperatures for many cold conditions were actually closer to nominal conditions.

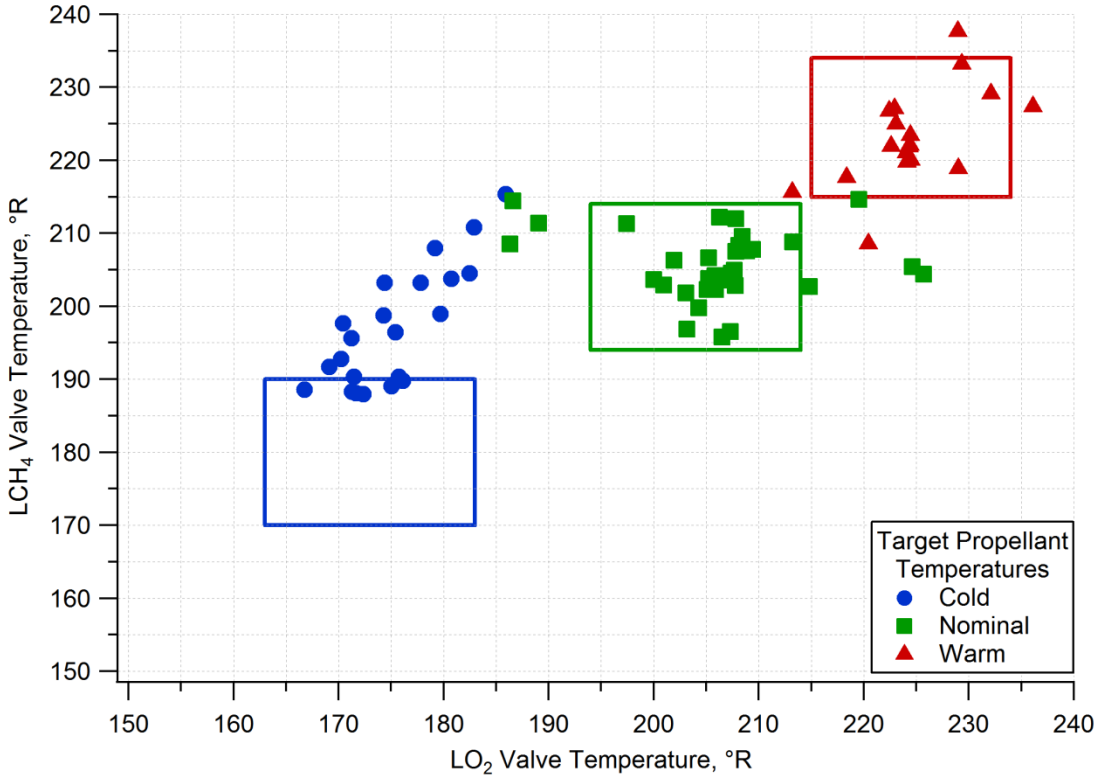

Figure 6. -- Plot of achieved propellant valve inlet temperatures and target ranges. Boxes represent target ranges.

With respect to the major objectives of the test series, Table II shows a table of the tested conditions with respect to pulse width (EPW) and duty cycle. The chart shows that the engine has been extensively tested over a wide variety of pulse widths and duty cycles, illustrating that it can operate over the range of duty cycles from 0 to 100 percent, as defined in objective (4), above.

Table II: Examined EPW and duty cycle combinations
(Aerojet [Sea-Level] = X; NASA Glenn =O; Both = ⊗)

EPW (ms)	Duty Cycle (%)							
	5	10	15	25	50	60	75	90
40	⊗		X	X				
50			X	X				
60	X		X	X		X		
80	⊗	X	X	⊗				
100	X		X	O	O			
120	X							
160	X	X	X	X				
320	X		X	X				
500					O			
960				X	X		X	X
1000				X	O			

The focus of GRC testing was minimum I-bit performance, so narrow EPW's and shorter duty cycles were used in the majority of the tests. Testing originally started at 50 percent duty cycle, but was changed to 25 percent and then 5 percent duty cycle after some coating degradation was observed on the columbium chamber. It is unclear whether the duty cycle was a definitive cause of the degradation, but a low duty cycle was retained to match pervious sea-level testing by Aerojet (Ref. 5). Since there was a programmatic requirement for a minimum EPW of 80 ms, the majority of testing at GRC focused on this EPW.

Figure 7 shows a plot of vacuum impulse bit versus pulse number for 80-ms EPW tests. The symbols are color-coded based on propellant temperature at the LO_2 (A) and LCH_4 (B) valve inlets. There is a dependency of impulse bit on valve inlet temperature, with colder propellants having higher impulse bits. Figure 8 also demonstrates this observation for tests which consisted of 30 pulses. The trend shows that increasing propellant inlet temperature decreases impulse bit. This is opposite of the trends observed in specific impulse testing, where increasing temperature led to increases in specific impulse and efficiency (Refs. 6,7).

Two factors, however, play a role in determining I-bit: (1) integration time, and (2) integration of thrust, both of which may be influenced by propellant temperature. Figure 9 is a plot of integration time (A) and peak thrust (B) versus the LO_2 valve inlet temperature. Integration time is highest with colder propellants, resulting in a higher I-bit. The corresponding colder hardware temperatures may lead to trapped liquid in the manifold, which would continue to vaporize after valve closure. Thus, chamber pressure takes longer to decay. This effect is also believed to cause a "double-pulse" phenomenon in some tests. Thrust, shown in Figure 9B, has a similar trend as integration time. Due to ringing in the thrust stand, these peak thrust values were based upon a curve fit profile, noted in the uncertainty analysis below. While a trend exists, it should be noted that the majority of the peak thrust data falls within a ±10- to 15-lb_f (±45- to 67-N) band, while oscillations observed in the thrust stand were as great as ±40 to 100 lb_f (±178 to 445 N), peak-to-peak. Thus it is difficult to claim a significant contribution to I-bit based upon thrust, and the cause of the I-bit trend can be primarily attributed to integration time. It should also be noted that average, nominal temperature I-bit values were consistent with values previously reported in Aerojet testing (Ref. 5), suggesting I-bit calculation methods are consistent.

With an EPW of 40 ms, the engine could achieve the MIB requirement of 4 lb_f-s (17.8 N-s) consistently, for a variety of propellant inlet temperatures. Figure 10 shows a plot of 40-ms EPW tests,

with the data points color mapped to propellant inlet temperatures. From the previous observed 80-ms EPW tests, warm tests generally have lower I-bit than cold tests. Thus it is not clear why a single warm data run shows such a significantly larger I-bit (≈40 percent) than colder tests at otherwise similar conditions. This set of data clearly defies trends observed, and is considered here as a statistical outlier. All of the other 40-ms EPW runs demonstrate a MIB of 4 lb_f-s (17.8 N-s) or less, which is consistent with prior Aerojet testing (Ref. 5).

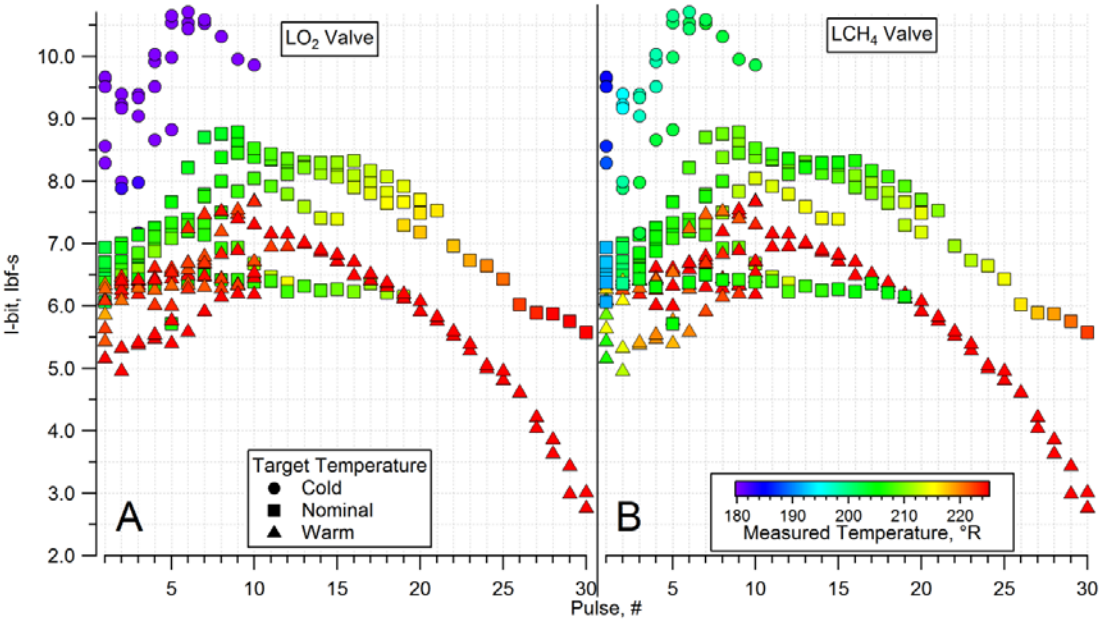

Figure 7.— I-bit for each pulse with propellant inlet temperature at the (A) LO_2 and (B) LCH_4 thruster valves. Only 80ms EPW runs with 1st pulse temperatures within ±10°R of the target are shown.

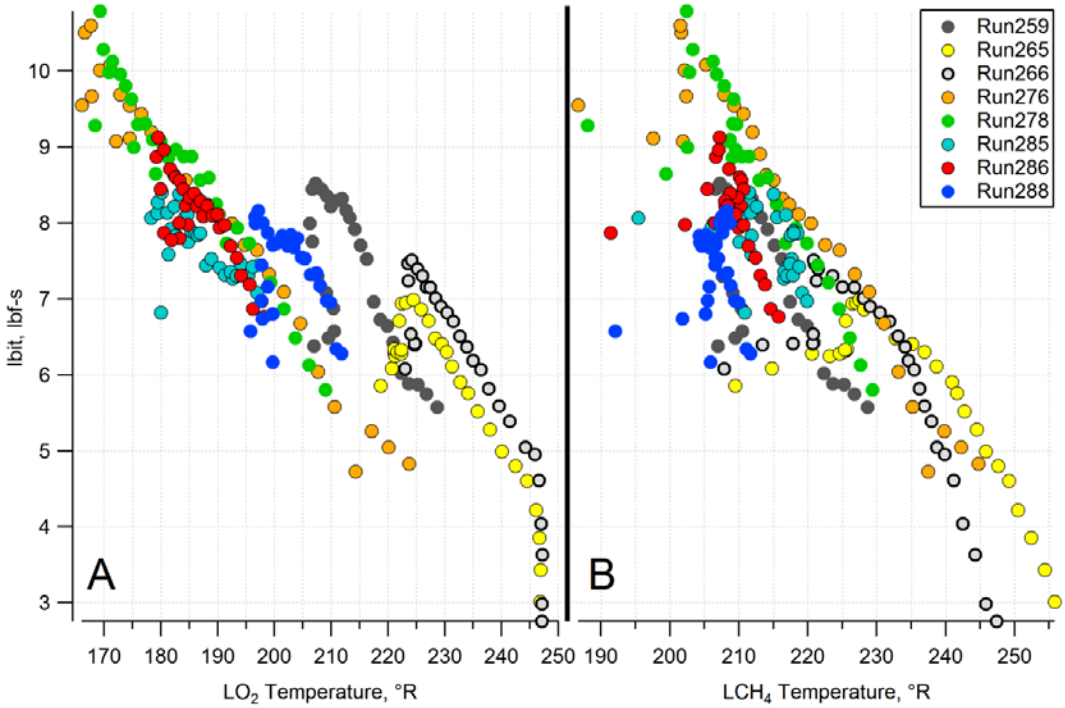

Figure 8.— I-bit as a function of (A) LO_2 and (B) LCH_4 inlet temperature for 30 pulse tests.

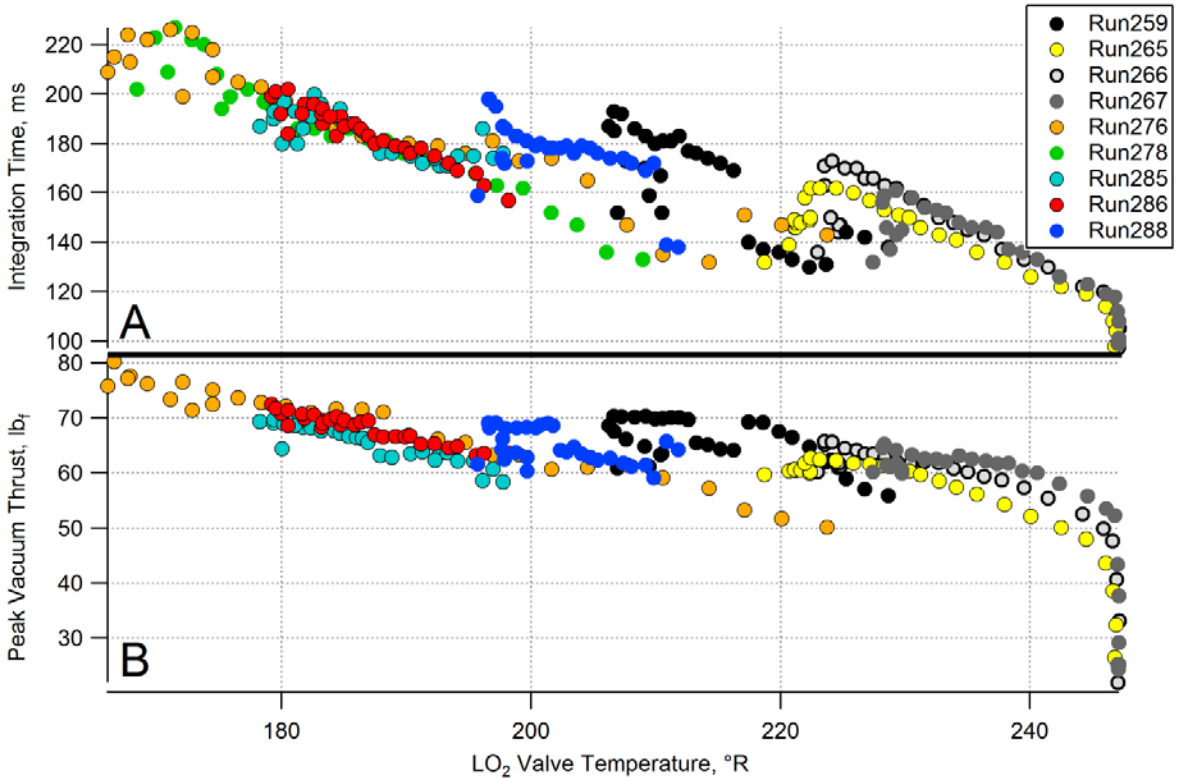

Figure 9. — The effect of LO_2 inlet temperature on (A) integration time and (B) peak thrust.

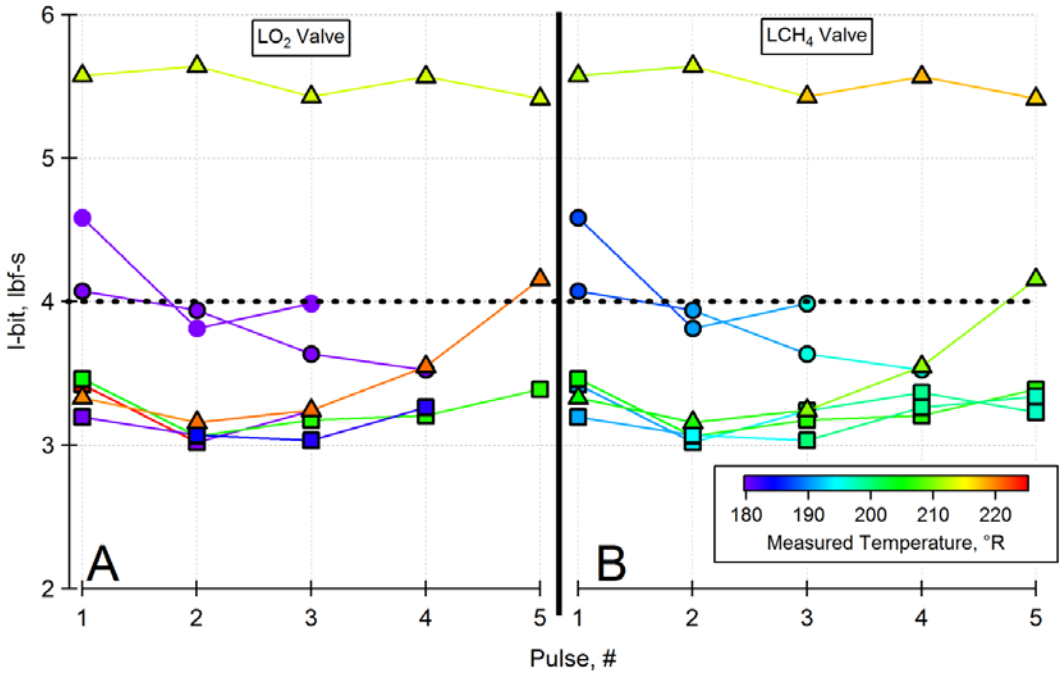

Figure 10.— I-bit for each 40ms EPW pulse with (A) LO_2 and (B) LCH_4 propellant inlet temperatures indicated by color. The dotted line indicates the minimum impulse bit target of 4 lb_f-s.

UNCERTAINTY ANALYSIS OF I-BIT

An uncertainty analysis was performed to qualify the I-bit values to fully meet JANNAF reporting standards (Ref. 16). The equations for I-bit and its uncertainty ($U_{\text{I-bit}}$) are:

$$\text{I-bit} = \int_{CH_4\ valve}^{10\%\ Pcav\ high} F_{vac}\, dt \tag{3}$$

$$U_{\text{I-bit}}^2 = \theta_F^2 B_F^2 + \theta_F^2 \mathcal{P}_F^2 + \theta_t^2 B_t^2 \tag{4}$$

In equation (3), F_{vac} is the vacuum thrust and t is the time. So, the thrust is integrated over the pulse width, as described above. In equation (4), B is the bias uncertainty which includes the instrumentation and calibration uncertainties, while $\mathcal{P}_F$ is the precision uncertainty which represents scatter in the data. Both also include a Student's t-distribution factor for a 95 percent confidence interval, and will be discussed in more depth below. The θ values are the sensitivity terms, which are the partial derivatives of I-bit with respect to its dependant variables (F, t). Simply they are: $\theta_F = t$ and $\theta_t = F_{vac}$. The bias uncertainty of time, B_t, is assumed to be negligible. The time stamp in the data files is taken from the data system clock. The bias uncertainty of the force term, $B_{\text{F}_{\text{vac}}}$, is derived from the vacuum thrust equation:

$$F_{vac} = K\left[\sum_{cells}^{3\ load} F + P_{amb}A_e\right] \tag{5}$$

$$B_{F_{vac}}^2 = \theta_F^2 B_F^2 + \theta_K^2 B_K^2 + \theta_{P_{amb}}^2 B_{P_{amb}}^2 + \theta_{A_e}^2 B_{A_e}^2 = K^2 B_F^2 + F^2 B_K^2 + A_e^2 B_{P_{amb}}^2 + P_{amb}^2 B_{A_e}^2 \tag{6}$$

where F is the force measured by the load cells, P_{amb} is the pressure outside the chamber, A_e is the exit area of the nozzle, and K is the calibration factor (calibrations are done at the beginning and end of each test day). The bias values were determined in the previous test program, and are displayed in Table III Table III. The previous program encompassed 55 tests, so the Student's t-distribution factor was 2 with a 95 percent confidence interval. The only term in Table III that would change with the current pulse test program is the sensitivity of the load cell calibration factor (K-factor), θ_K. As shown in equation (6), this term is equal to the average force exerted on the load cells over all tests. For the previous program (Ref. 7) it was ≈100 lb_f (445 N), for the pulse program it was ≈50 lb_f (222 N) in each pulse. Using the latter would decrease the bias error, $B_{\text{F}_{\text{vac}}}^2$, to a value of approximately 13.3. However, the uncertainty calculations were programmed prior to the pulse test program so estimates could be obtained in real time. So, while the values in Table III are somewhat conservative, they were retained.

Table III: The bias uncertainty for the vacuum thrust measurement is shown.

	Sensitivity	$b_{Instrument}$	$b_{Calibration}$	$B^2=\Theta^2\ \Sigma(tb)^2$
Force (summation of 3 load cells)	$1.033=\theta_F$	±1 lb_f each	±0.06 lb_f each	12.862
Force calibration term (K factor)	$99.863=\theta_K$	-	0.005	0.999
Thrust - Area, exit	$0.210=\theta_A$	±0.001 in^2	-	1.757×10^{-7}
Thrust - Pressure Ambient	$13.710=\theta_P$	±0.015 psi	0.0063	0.204
			$B_{\text{F}_{\text{vac}}}^2$	14.065

The precision uncertainty, $\mathcal{P}_F$, is typically based on the standard deviation. However, the thrust is not steady in these short (80-ms) pulse durations, resulting in a bell shaped curve over time. There is also a great deal of ringing seen in the thrust data. Using a simple average thrust value in the standard deviation calculation is not representative, since it neglects this time dependency. Therefore, a polynomial curve fit was used to predict a smooth, time dependant thrust response for each pulse. The standard error of the predicted values was used to determine the precision uncertainty. Figure 11 shows thrust

data and the curve fit for two pulses during a pulse train with warm propellant conditions. Ringing in the load cell causes significant fluctuations in the thrust, resulting in significant uncertainty values. Figure 11A was the worst in this particular train with high amplitude fluctuations (≈40 to 100 lb_f (178 to 445 N), peak-to-peak). This resulted in a poor curve fit and high error values. Thus, the total uncertainty of the I-bit was high. In Figure 11B the amplitude of the thrust fluctuations were lower (≈20 to 40 lb_f (89 to 178 N), peak-to-peak), so the standard error and the resulting I-bit uncertainty were also lower.

Note that the transient nature of the short pulse durations is the primary factor in these uncertainties. Since the chamber pressure profile should trend the same as thrust, it was substituted into the I-bit equation. Without the oscillations on the thrust stand the resulting "P_c-bit" should have a lower uncertainty than its thrust-based counterpart. However, the improvement was only a 5-10 percent reduction in uncertainty. The polynomial curve fit used here to estimate the precision uncertainty is not an optimal prediction of the transient effects. The bias uncertainty, which is time independent, is typically 8.5 percent on I-bit and 3.5 percent on P_c-bit. These are conservative uncertainties, but are a more accurate representation of the facility capabilities.

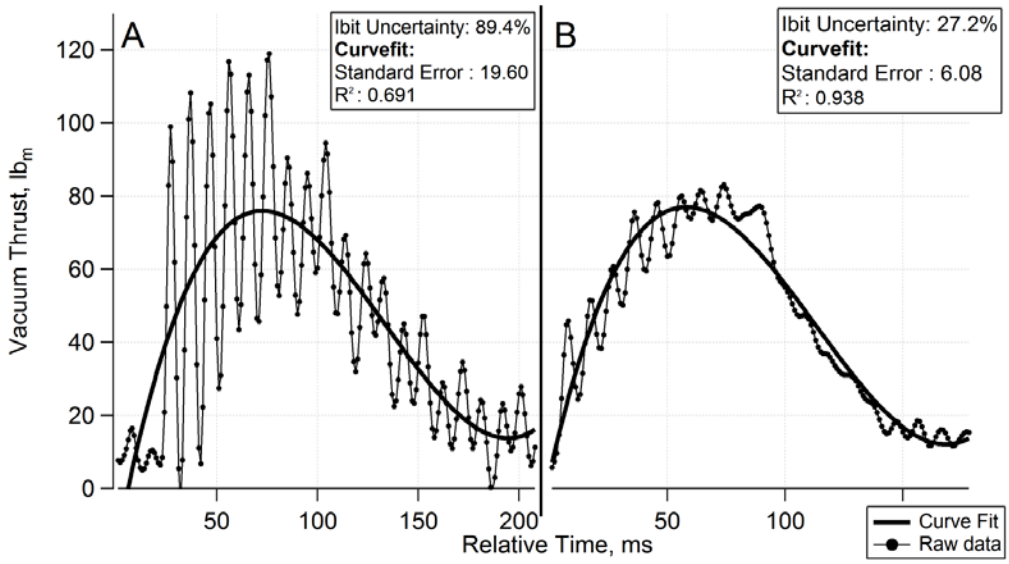

Figure 11.— Thrust curves for two pulses from a test at warm propellant conditions. The solid line indicates the polynomial curve fit used to estimate the thrust precision uncertainty for ((A) worst case and (B) best case thrust fluctuations.

DOUBLE PULSE PHENOMENON

A unique phenomenon was observed whereby the pulse regained strength after the valves had closed, as indicated visibly by a second flame pulse. This "double pulse" is best described using Figure 12, which shows a sequence of video images from a burn. The nominal, main pulse is shown in images 1 to 6, but in image 7 the flame regains strength. While the duration of the secondary pulse varies, this figure is representative of the behavior. Secondary pulses are not fully expanded and have a more disperse flame. However, from the pressure traces shown in Figure 13, the secondary pulses do not correspond to a significant secondary rise in chamber pressure, but rather slower pressure decay. Because the video frame rate is only 30 Hz, the visualization of the phenomena could not be directly correlated with the 1000-Hz data.

One possible cause of the double pulse is suggested in Figure 14. The propellant temperatures in the manifold for both fuel and oxidizer are shown in Figure 14A. The methane temperature behavior remains consistent throughout the test. But at 12 s (pulse 8) the oxygen temperature plummets, crossing over to a saturated state in the highlighted region of the graph. Figure 14b shows the corresponding oxygen manifold pressure. When there is liquid in the manifold, the pressure fails to return to its zero

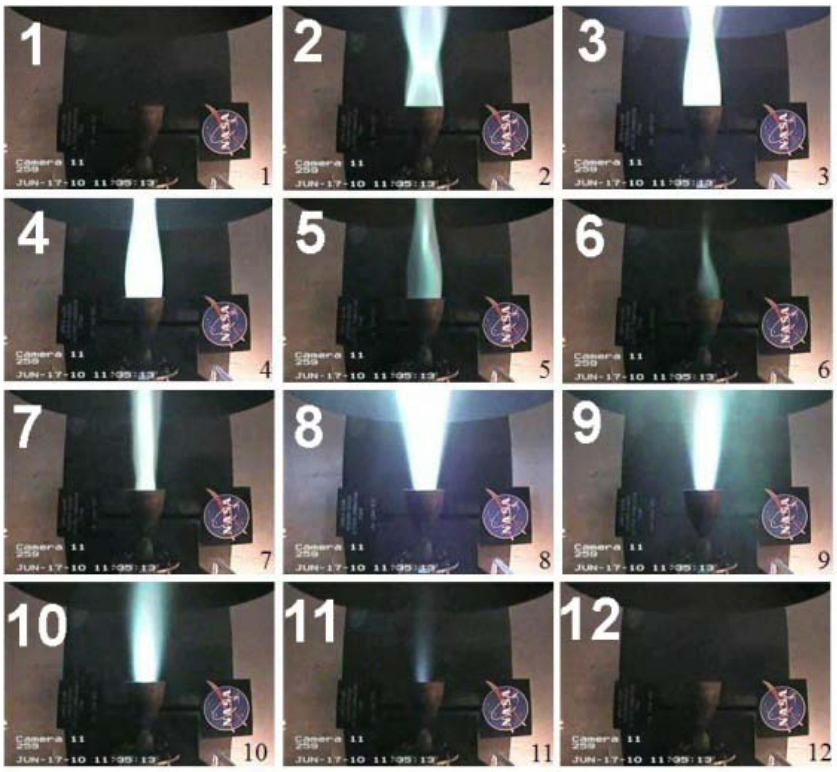

Figure 12.— Image sequence illustrating the double pulse phenomena. The main pulse is shown in images 2 to 6, and the secondary “double” pulse begins in image 7.

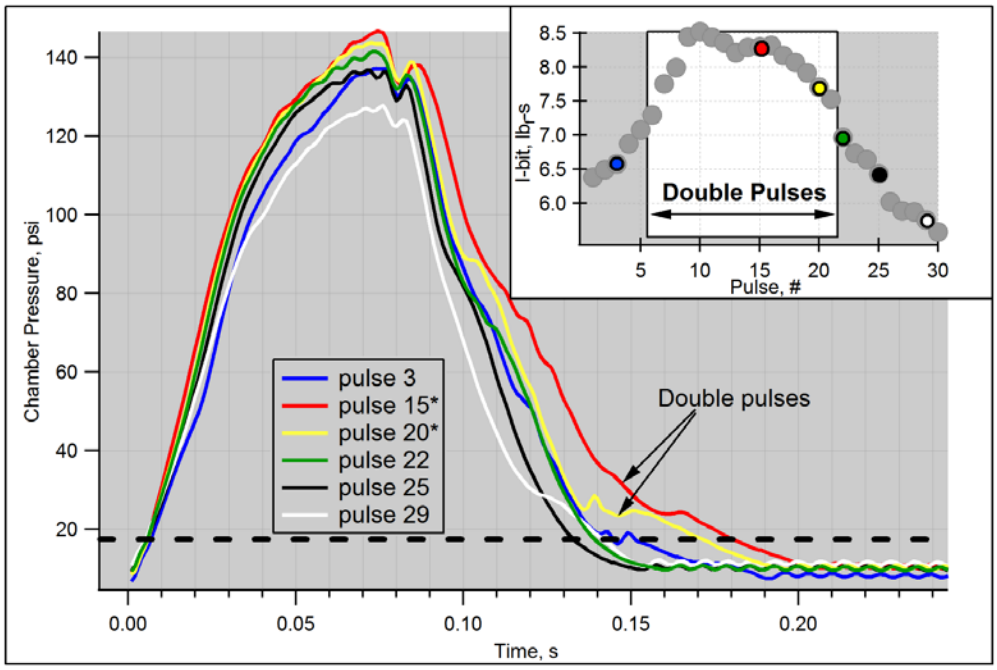

Figure 13.— Chamber pressures several pulses (overlaid) of a 30-pulse train with I-Bits shown in the graph inset. The pressure decay for the double pulses (pulses 15 and 20) is slower, leading to a longer integration time for I-bit.

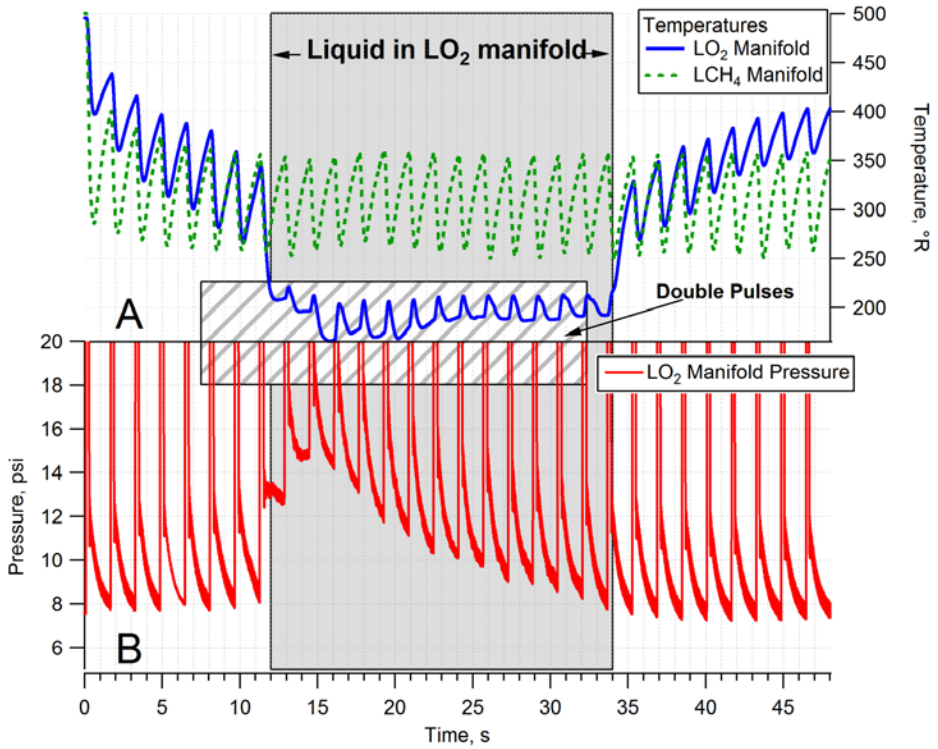

Figure 14.— Saturation in the LO_2 manifold is indicated in the (A) manifold temperature and (B) LO_2 manifold pressure. Double pulses (box) overlap this saturation region.

value between pulses. This could be a result of liquid oxygen vaporizing in the manifold after the oxygen valve has closed. Since the methane valve closes 40 ms after the oxygen, both reactants are present in the chamber. Thus a flame could continue, or reignite, after the oxygen valve was commanded closed. It should be noted that, the double pulse region does not exactly correlate with the saturation region in Figure 14. This temperature is only a point measurement taken at the entrance to the manifold, and elsewhere in the manifold system the temperature may be such that propellant exists in a different state then indicated by the manifold instruments.

Figure 15 illustrates the effect of the propellant temperature conditions on this phenomenon, indicated in the title of each plot. The oxygen manifold temperature is shown for all 9 tests with 30-pulse pulse-trains. The highlighted region is where double pulsing was observed. The darker colored portions of the temperature traces indicate saturation (calculated using the manifold pressure at each point). The double pulse phenomenon is most prominent in the cold and nominal tests, where the majority of the 30 pulses showed double pulsing. This is supported by the temperature traces which indicate that the oxygen is liquid in the manifold for the much of these tests. There is fluctuation between liquid and gas for several tests, such as Run 285, which may suggest a two-phase or borderline condition. In contrast, double pulses are infrequent during tests at warm propellant conditions. While the data suggests the liquid is in a saturated state in the manifold, the temperature shifts are more severe, perhaps indicating that the propellant is experiencing different bulk conditions than the localized thermocouple indicates. Another feature was observed in conjunction with the double pulsing; the pulses began to grow weaker, as evident by lower I-bits, after the double pulsing had subsided. Visually, these appeared to be shorter lived than pulses early in the train (prior to the double pulsing), and also lower peak chamber pressures, as seen in Figure 13. The weakened pulses correspond to the continued temperature rise in the manifold causing a transition to gas.

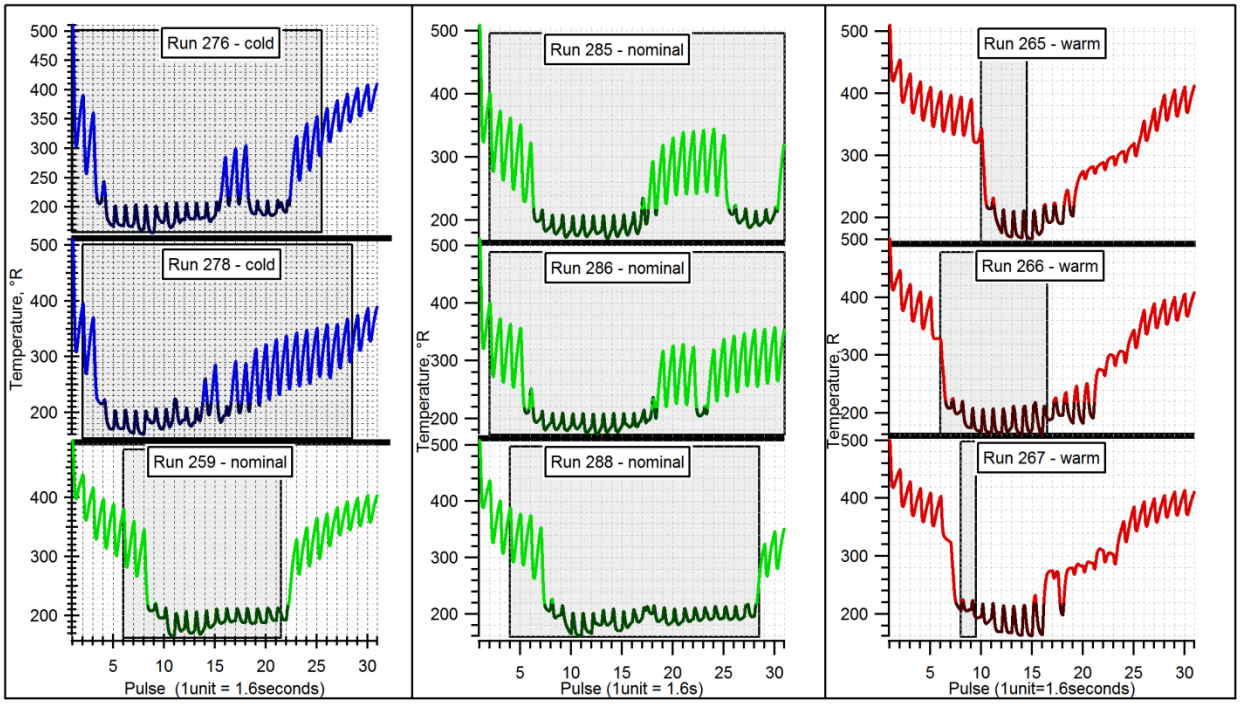

Figure 15.— The LO_2 manifold temperatures are plotted for each 30-pulse train run. Double pulses were observed in the highlighted areas, and the darker color of the trace indicates the temperature is below the saturation condition.

TEMPERATURE RISE IN FEED SYSTEM

The I-bit trends, along with the weak pulse phenomena, are related to propellant warming. This warming trend is counterintuitive; one would expect the hardware to cool while cryogenic propellants are flowing through the system. (Note that the effect of this temperature rise on I-bit performance is represented in Figure 8). Temperature measurements along the inlet lines are plotted in Figure 16, with the locations indicated in the schematic. The valve temperatures show some initial instability before steadily rising. The two upstream locations, venturi and flow meter 1, show steady or shallow slopes during the valve instability, and then begin to rise with the valve temperature. However, the location between the two turbine flow meters is unique. The temperature is higher than any of the others, and the increase occurs here first. (The vertical lines indicate the slope rise of this flow meter temperature and valve temperature). Thus it appears that the heat rise initiates at this location. This may be due to recirculation or poor rotation of the turbine flow meter. During previous specific impulse testing (Ref. 6,7), observed pressure transients were also traced to this location. This flow meter was removed after the pulse testing, but subsequent tests for validation of this theory have yet to be completed.

While engine heat soak back has not been definitively ruled out as a contributor, it is an unlikely factor in the temperature rise for two reasons. First, the flow meters are not in direct line of sight of the engine nozzle. If soak back was a factor, components in direct line of sight or connected to the engine, such as the valves, should see heat rise first as expected from radiative or conductive principles. Secondly, in the later pulses the engine throat does not radiate as brightly, suggesting the chamber is not experiencing as much heating from combustion (either from cooler flame or better wall cooling). Yet, there is no indication from the temperature plots that the heating of the lines has subsided.

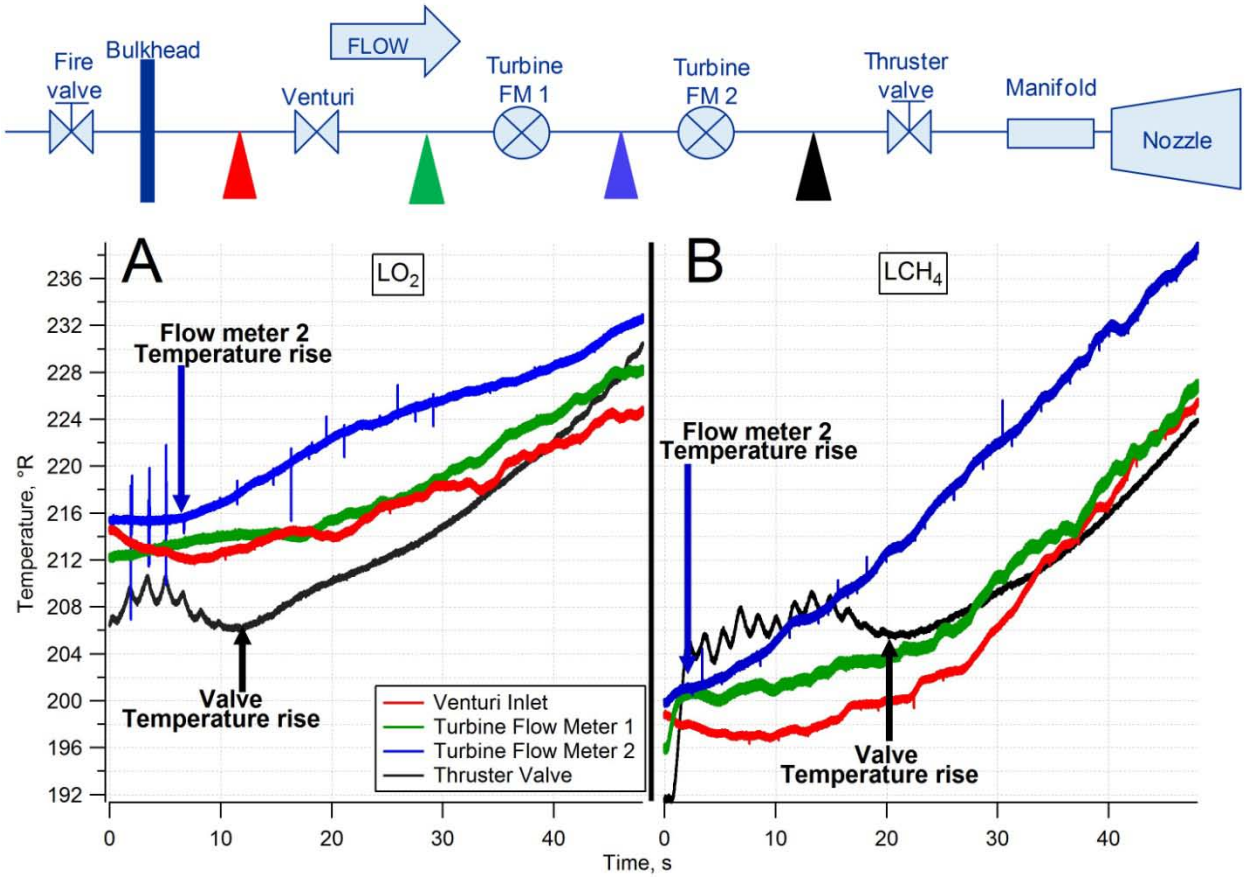

Figure 16.— Feed system temperatures for (A) LO_2 and (B) LCH_4 lines. Corresponding sensor locations are show in the above schematic.

Another source of potential warming in the propellant lines was the trace cooling and propellant bleed lines. These lines circulated liquid argon or liquid nitrogen around the propellant lines to thermally condition the propellant prior to a run. This cooling system was manually adjusted to meet test needs such that trace cooling may have been on or off for a given run. Using bleed valves in the propellant lines, a portion of the propellant could also be vented just upstream of the thruster valves as a means of maintaining propellant line temperature. These valves were closed for zone 2, and thus the non-flowing propellant during the dwell portions of zone 2 would be susceptible to line warming. Since the turbine flow meters were large masses relative to the rest of the propellant lines, it is likely that heating would begin in this vicinity. Additional insulation was installed following this test series as a further precaution against propellant warming.

SUMMARY AND CONCLUSIONS

The 100-lb_f LO_2/LCH_4 RCE developed by Aerojet was tested to determine I-bit performance. All experiments took place in a reduced pressure environment using the Altitude Combustion Stand at the NASA Glenn Research Center. Propellant temperature was varied between three set point conditions to simulate operation limits of an in-space system. Pulse train length (number of consecutive pulses), pulse duration (EPW), and duty cycle were all adjusted to meet test needs.

The performance fully met three of the four objectives set forth: It was operated at, and below, the required minimum pulse duration of 80 ms; it achieved a minimum impulse bit (MIB) of less than 4 lb_f-s (at 40-ms pulse duration); and it was operated at a range of duty cycle conditions. The fourth requirement stated that the MIB repeatability should be within ±5 percent after achieving stable temperature. However, stable temperatures were not achieved due to warming in the lines, believed to

be associated with one of the turbine flow meters, though this has yet to be confirmed. This was a facility issue, and not related to the performance of the engine. As a result, propellant temperatures increased gradually over the pulse train, which involved as many as 30 consecutive pulses. The I-bit values were shown to be strongly dependant on propellant inlet temperature, with warmer propellants showing shorter I-bits. Thus the I-bit values dropped off toward the end of longer pulse trains. The number of consecutive pulses demonstrates reliable and repeatable ignition and pulse performance, bolstering the feasibility of this propellant combination for future exploration endeavors.

Several issues with this particular engine system did occur. A unique phenomenon was observed whereby the engine reignited immediately after the values were closed, resulting in a “double” pulse. Manifold temperature and pressure conditions indicate that this may have been due to a two phase flow condition. Vaporization of liquid in the oxygen manifold could have reacted with the lagging methane flow to cause a short re-ignition. This double pulse phenomenon also led to higher impulse bits (due to longer integration times).

PLANNED FUTURE WORK

Testing with this engine should continue with a focus on ignition phenomena. Since one of the perceived drawbacks of this propellant combination is high ignition energy, this program should strive to determine energy limits. A well instrumented exciter unit should be used to obtain high fidelity voltage information of the spark discharge. By coupling this to the existing pressure instruments, it should be possible to determine the energy of the ignition spark. A variable energy exciter unit has already been developed to explore these limits.

ACKNOWLEDGEMENTS

The authors greatly acknowledge the entire facilities team which operated the ACS facility and made testing possible. Additionally, the support received by the NASA Glenn Materials Branch is also appreciated, as well as discussion and insight provided by the engine manufacturer Aerojet. This work was supported by the Propulsion and Cryogenic Advanced Development (PCAD) project with which is part of the NASA Exploration and Technology Development Program (ETDP).

REFERENCES

1. Melcher, J.C. and Allred, J.K., "Liquid Oxygen/Liquid Methane Testing of the RS-18 at NASA White Sands Test Facility", AIAA 2008-4843, *44th AIAA/ASME/SAE/ASEE Joint Propulsion Conference and Exhibit,* Hartford, CT, July 21-23, 2008.

2. Melcher, J.C. and Allred, J.K., "Liquid Oxygen/Liquid Methane Test Results of the RS-18 Lunar Ascent Engine at Simulated Altitude Conditions at NASA White Sands Test Facility", AIAA 2009-4949, *45th AIAA/ASME/SAE/ASEE Joint Propulsion Conference and Exhibit,* Denver, CO, August 2-5, 2009.

3. Over, A.P., Klem, M.K., and Motil, S.M., "A Successful Infusion Process for Enabling Lunar Exploration Technologies", AIAA 2007-6196, *AIAA Space 2007 Conference and Exposition,* Long Beach, CA, September 18-20, 2007.

4. Stone, R., Tiliakos, N., Balepin, V., Tsai, C.-Y., and Engers, R., "Altitude Testing of LOX-Methane Rocket Engines at ATK GASL", AIAA 2008-3701, *26th AIAA Aerodynamics Measurement Technology and Ground Testing Conference,* Seattle, WA, June 23-26, 2008.

5. Robinson, P.J., Veith, E.M., Hurlbert, E.A., Jimenez, R., and Smith, T.D., "100-lb_f LO2/LCH4 - Reaction Control Engine Technology Development for Future Space Vehicles", *59th International Astronautical Federation,* Glasgow, Scotland, United Kingdom, September 29 - October 3, 2008.

6. Marshall, W.M. and Kleinhenz, J.E., "Hot-Fire Testing of 100 lb_f LOX/LCH_4 Reaction Control Engine at Altitude Conditions", *JANNAF 57th JPM/7th MSS/5th LPS/4th SPS Joint Subcommittee Meeting,* Colorado Springs, CO, May 3-7, 2010.

7. Marshall, W.M. and Kleinhenz, J.E., *Performance Analysis of Specific Impulse Tests of a 100-lbf (445-N) LO2/LCH4 Reaction Control Engine at Altitude Conditions*, NASA TM-2011-217131, National Aeronautics and Space Administration, Cleveland, OH, 2011.

8. *The Historic Rocket Engine Test Facility*, Produced by: NASA GRC, Available from: http://retf.grc.nasa.gov/, Last Accessed 2011.

9. Smith, T.A., Pavli, A.J., and Kacynski, K.J., "Comparison of Theoretical and Experimental Thrust Performance of a 1030:1 Area Ratio Rocket Nozzle at a Chamber Pressure of 2413 kN/m^2 (350 psia)", AIAA-87-2069, *AIAA/SAE/ASME/ASEE 23rd Joint Propulsion Conference,* San Diego, CA, June 29 - July 2, 1987.

10. Pavli, A.J., Kacynski, K.J., and Smith, T.A., *Experimental Thrust Performance of a High-Area-Ratio Rocket Nozzle*, NASA TP-2720, National Aeronautics and Space Administration, Cleveland, OH, 1987.

11. Grasl, S.J., Skaff, A.F., Nguyen, C., Schubert, J., and Arrington, L., "Liquid Methane/Liquid Oxygen Propellant Conditioning and Feed System (PCFS) Test Rigs - Preliminary Test Results", *JANNAF 57th JPM/7th MSS/5th LPS/4th SPS Joint Subcommittee Meeting,* Colorado Springs, CO, May 3-7, 2010.

12. Skaff, A., Grasl, S., Nguyen, C., Hockenberry, S., Schubert, J., Arrington, L., and Vasek, T., "Liquid Methane/Liquid Oxygen Propellant Conditioning Feed System (PCFS) Test Rigs", *JANNAF 3rd Spacecraft Propulsion System Joint Subcommittee Meeting,* Orlando, FL, December 8-12, 2008.

13. *DIAdem: Getting Started with DIAdem*, National Instruments, Austin, TX, 2009.

14. Lemmon, E.W., Huber, M.L., and Mclinden, M.O., *NIST Standard Reference Database 23: Reference Fluid Thermodynamic and Transport Properties-REFPROP, Version 8.0*, National Institute of Standards and Technology, Standard Reference Data Program, Gaithersburg, MD, 2007.

15. Stiegemeier, B.R. and Marshall, W.M., "Sea-Level Testing of a 100 lb_f LOX/Methane Reaction Control Engine", *JANNAF 57th JPM/7th MSS/5th LPS/4th SPS Joint Subcommittee Meeting,* Colorado Springs, CO, May 3-7, 2010.

16. *JANNAF Rocket Engine Performance Test Data Aquisition and Interpretation Manual*, CPIA Publication 245, Chemical Propulsion Information Agency, Silver Spring, MD, 1975.